Penerbit Akademia Baru

Journal of Advanced Research in Fluid Mechanics and Thermal Sciences

Journal homepage: www.akademiabaru.com/arfmts.html
ISSN: 2289-7879

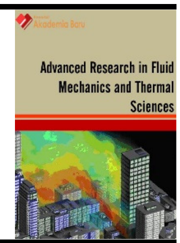

Evaluation of a Large Eddy Simulation on Thermal Boundary Condition in Underground Car Park

Open Access

Ahmad Faiz Tharima[1,2,*], Mohd Zamri Yusoff[2], Md Mujibur Rahman[2]

[1] Fire and Rescue Department of Malaysia, Lebuh Wawasan Presint 7, 62250 Putrajaya, Malaysia
[2] College of Engineering, Universiti Tenaga Nasional, Jalan IKRAM-UNITEN, 43000 Kajang Selangor, Malaysia

ARTICLE INFO

Article history:
Received 7 May 2018
Received in revised form 4 July 2018
Accepted 23 July 2018
Available online 12 August 2018

Keywords:
Adiabatic, critical Velocity, underground car park

ABSTRACT

Both Fire Dynamic Simulator (FDS) and Smokeview (SMV) were adopted to predict the heat distribution and the smoke propagation. The data are important for determining the required tenability limit in an underground car park during fire. The credibility of FDS result depends heavily on the numerical setting and the imposed boundary conditions. The present study explored the influence of different thermal boundary conditions, i.e. adiabatic and constant wall temperature boundary conditions. The grid-independent Heat Release Rate (HRR) and the vertical temperature profiles on some selected locations were firstly obtained. It was found that the R^2 of the constant temperature thermal boundary condition was the highest (89.4%). Meanwhile, the R^2 of the adiabatic thermal boundary condition was 87.5%. Therefore, the constant wall temperature boundary condition was adopted for subsequent analysis. On the other hand, the temperature distribution was dependent on the imposed thermal boundary condition as well. For adiabatic condition, the smoke took lesser time to reach the floor. However, for constant temperature boundary condition, the smoke layer remained at the upper level and the smoke concentration was low near the end wall. Also, the predicted critical velocity for the case of constant temperature boundary condition was much lower than that of adiabatic boundary condition. In general, lower critical velocity indicates that the hot gases would reside at the upper level longer.

1. Introduction

At current, there are many types of smoke back layering control. For instance, the smoke backflow can be prevented if the air velocity is sufficiently large [1]. In contrast, some authors indicated that the airflow velocity should be kept as low as possible in order to maintain the smoke stratification and to keep the downstream smoke-free [2]. There are many definitions on smoke-free nevertheless. Accordingly, smoke back layering is negligible when smoke is not detected at upstream [3] or downstream [4]. Thus, the effect of critical velocity is more apparent when there is no smoke back layering [4].

* *Corresponding author.*
E-mail address: pait.afz@gmail.com (Ahmad Faiz Tharima)

The critical velocity is usually measured at the target location where the smoke back layering is expected. Meanwhile, the horizontal velocity is measured at the air inlet [3,5–7] such as near the jet fan (forced ventilation) or the window (natural ventilation). The different of both forced and natural ventilation is proven to have a linear correlation to smoke back layering distance [5].

The degree of smoke back layering is dependent on factors such as ventilation velocity, tunnel surface condition, size of modelled fire source and obstacles near the fire source [8]. Moreover, the critical velocity in the case of transverse beams is much lower than that of parallel beams. Therefore, the jet fan in the former case is relatively smaller [6].

The critical velocity may differ due to the imposed boundary conditions. Owing to the fact that not all information were available while designing the CFD model [9], sensitivity analyses on several critical model setup parameters were performed to grasp better understanding on how the tenability limit would vary during fire in the future study. These critical parameters were ceiling height, beam span length, transversal beam depth, longitudinal beam depth and extraction fan rate [3,10–23]. In the current work, FDS was used to assess the effects of both boundary conditions.

2. Methodology

2.1 CFD Simulation

The computational fluid dynamics (CFD) simulation was performed by using FDS software, which is a specialized software in modelling fire-driven fluid flow. Flow turbulence was modelled via Large Eddy Simulation. Table 1 shows the numerical settings of the simulation.

Table 1
The numerical setting for simulation

Parameter	Numerical setting
Geometry dimension	4m x 1.6m x 0.3m
Mesh size	0.94cm
HRRPUA	234.5kW/m^2
Fuel	Methane (CH_4)
CO yield	0.2
Soot yield	0.07
Hydrogen Fraction	0.1
Fire source area	0.2m x 0.2m
Ambient temperature	28.95
Relative Humidity	65
Combustion model	default mixture fraction combustion
Turbulence model	standard Smagorinsky LES, C_D=0.20

2.2 Boundary Condition

Two different thermal boundary conditions were considered in the CFD model, i.e. adiabatic wall and constant wall temperature boundary conditions. The surrounding environment was however not modelled. In this condition, the ambient temperature was fixed at 28.95^{o}C whereas the wind effects were not taken into account. The two longitudinal beams placed at the center of car park were supported by transversal beams and columns of various sizes.

2.3 Grid Refinement and Validation

The CFD models were discretized by using meshes of different sizes, i.e. 3.57 cm, 1.47 cm and 0.94 cm. The numerical results were then compared with the experimental data provided by Ji *et al.,* [18]. Figure 1 shows the temperature values at 0.01m below the ceiling. The result converged to the maximum temperature as the grid was refined. Table 2 shows the FDS and experimental results. As seen, in the table, the error decreased as the grid size was reduced. It was interesting to note that the error was merely 4.33% at the finest mesh level. As shown in Figure 1, the coefficient of determination (R^2) for the finer mesh case (i.e. 87.9%) was quite similar to those of cases employing moderate and coarse meshes. Therefore, the FDS results obtained on the finer mesh could be regarded as grid-independent.

Figure 2 shows the geometry of the enclosed car park (i.e. located at the Simulator Building at the Fire and Rescue Academy of Malaysia). The CFD model was scaled down 10 times while preserving the dimensionless numbers such as Froude number, Prandtl number and Reynold number [22,23]. The results were obtained on mesh layouts of various sizes; 5.44 cm, 2.18 cm, 1.36 cm and 0.94 cm.

As reported in Figure 3, the HRR values obtained on mesh layouts of sizes 1.36 cm and 0.94 cm were quite similar. Therefore, the grid size of 0.94cm was selected for subsequent analysis. Also, the grid refinement factor $r = h_{coarse}/h_{fine}$ of >1.3 was considered desirable (see Table 3) [24].

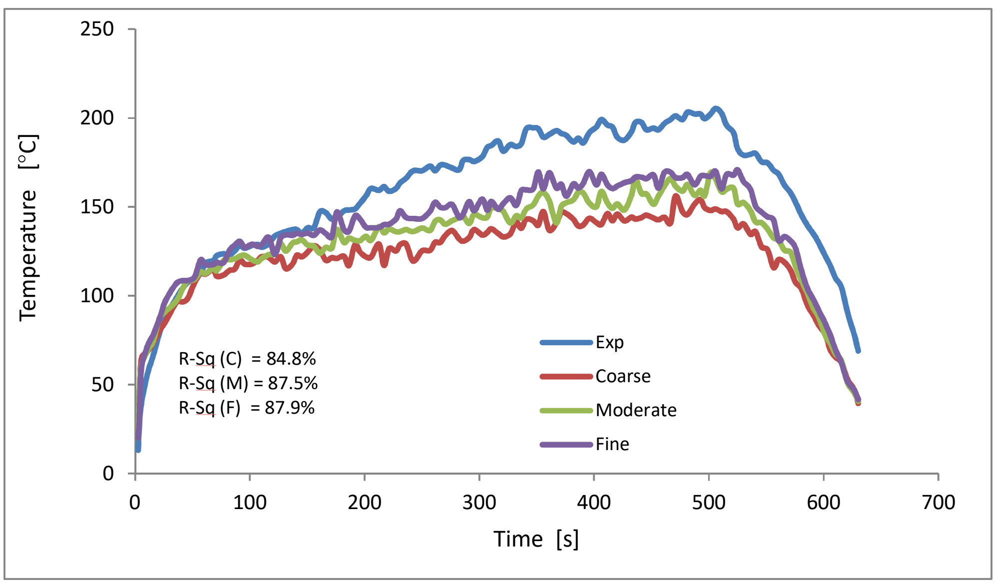

Fig. 1. Temperatures at thermocouple tree A

Table 2
Relative difference of maximum temperature between experimental result and model prediction

Mesh size	Number of cells	Maximum temperature [°C]		Relative error
		Experiment	FDS	
3.57	32,928		166.33	19.01%
1.47	471,648	205.38	189.95	7.51%
0.94	1,797,760		196.48	4.33%

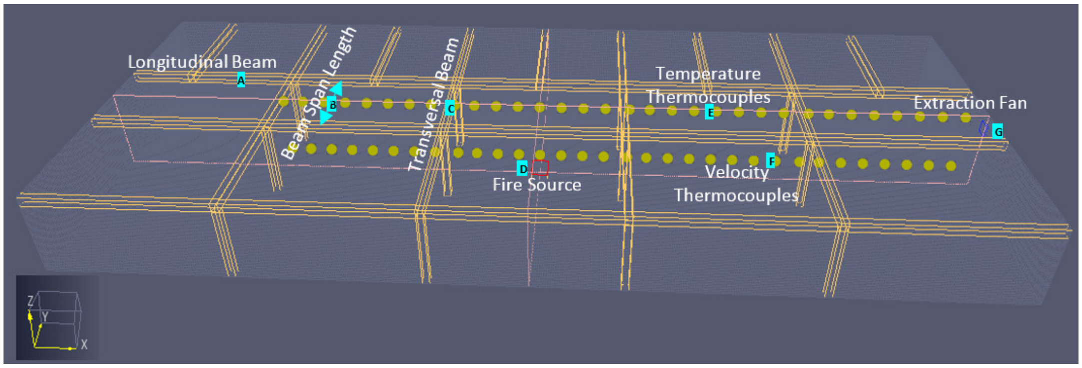

Fig. 2. An underground car park geometry

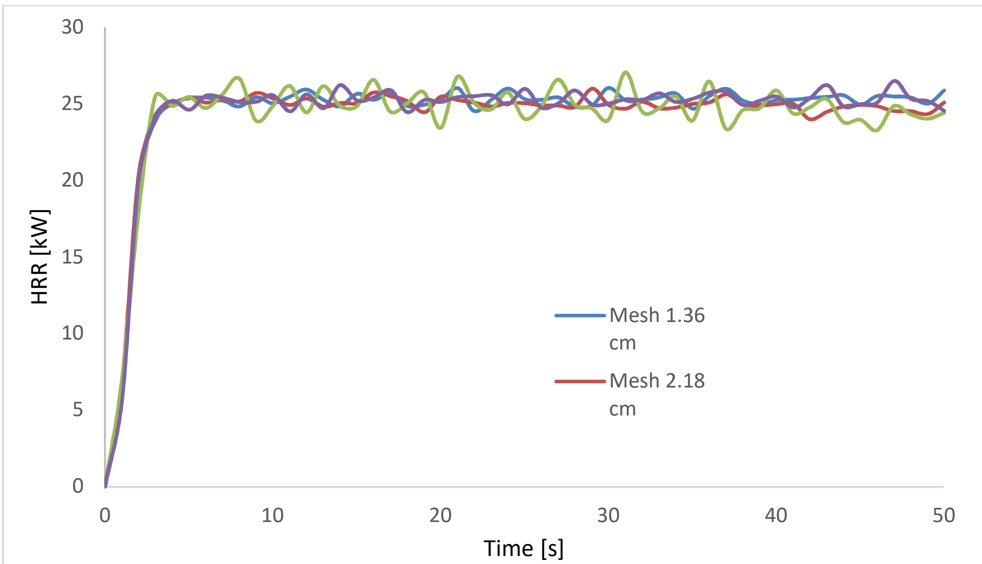

Fig. 3. Heat release rate in difference meshes

Table 3
Grid refinement factor

Mesh size	Number of cells	Grid refinement factor '*r*'
5.44cm	15360	-
2.18cm	240000	2.3
1.36cm	983040	1.5
0.94cm	2312000	1.3

3. Results

3.1 Heat Release Rate

Here, both boundary conditions were imposed and their effects on the numerical results were studied. The heat release rate of 9.38 kW was imposed according to experiment investigated by Ji *et al.,* [18]. Figure 4 indicates that the constant thermal boundary condition has higher R^2 (89.4%) as compared to that of the adiabatic thermal boundary condition (87.5%). It indicates that the highest temperature is obtained at the constant temperature boundary condition which gives the maximum heat transfer [25]. The highest measured temperature is expected to have influenced on velocity as well as smoke concentration which represents the actual problem accordingly. Therefore, it was believed that the constant wall temperature boundary condition could be used for subsequent analysis.

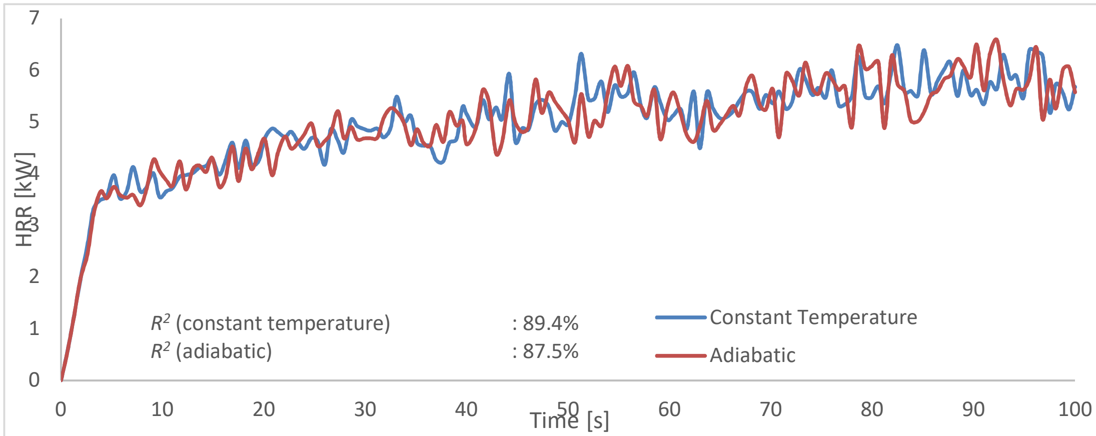

Fig. 4. Heat release rate

3.2 The Effect of Underground Surface Condition on Smoke Level

The residence time of smoke at the upper level is dependent on the type of boundary condition. The smoke concentration (at the symmetry plane) is shown in Figure 5. From Figure 5, in the case of adiabatic condition, the smoke took lesser time to reach the floor. Therefore, the tenability condition in the underground car park was not fulfilled. Nevertheless, for the case of constant temperature boundary condition, the smoke remained at the upper level and the smoke concentration was found to be low near the end wall due to the heat transfer to the end wall. According to the numerical simulation, it shows that the smoke reached to the floor level at approximately 103s by using the boundary condition of constant temperature while it is vice versa for the adiabatic condition where the smoke reached to the floor earlier. Based on this, all occupants have enough time to reach a place of safety. In the later intensive study, this boundary condition is found to be most appropriate for studying the required safe escape time.

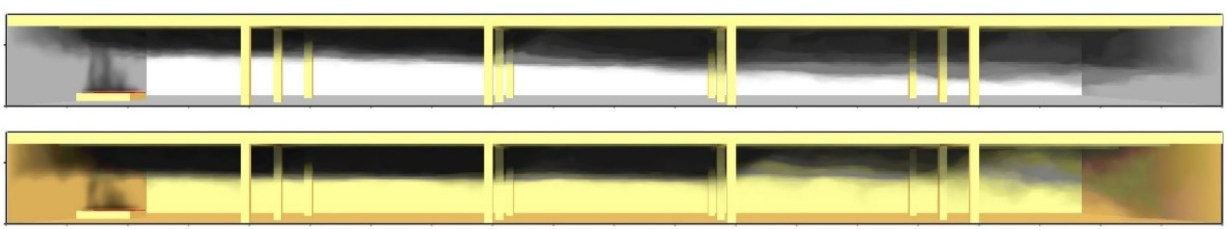

Fig. 5. The different smoke concentration at the upper level and near the end wall. Top: adiabatic, bottom: constant temperature.

3.3 Temperature Distribution

The temperature field would vary accordingly due to the difference in wall thermal boundary conditions. For adiabatic condition, the temperature near the ceiling was higher. Apparently it caused the smoke to reach the opposite direction due to the buoyancy effect. For the constant temperature boundary condition, the buoyancy effect is minimal. Therefore, the smoke was concentrated at the fire source as well as the downstream region (Figure 6).

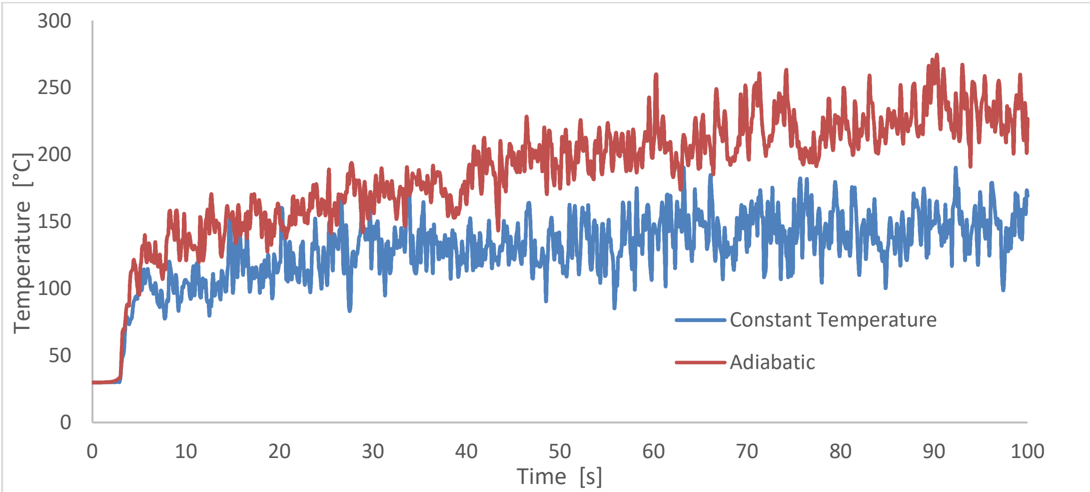

Fig. 6. Temperature recorded above a fire source

3.4 Critical Velocity

The influence of critical velocity on the smoke layer was studied with a bit differing of numerical setting. Here, the angular position of the transversal beam was varied between 30° and 65° [26]. The longitudinal beam depth was set larger than that of the transversal beam so that the smoke flow could be channeled to the exhaust fan.

The fire source (0.0762 m x 0.11684 m) was placed at the center of the car park compartment. The fuel source considered was propane. The carbon monoxide and soot yields were prescribed as 0.05 and 0.024, respectively. The value of 8 MW was chosen by considering possible failure in the sprinkler system [27]. Because scaling relations is used, the fire size was scaled down to be 25.3kW, resulting in 2842.7 kW/m^2 heat flux [28]. Whereas the exhaust fan rate was set at 0.31 m^3/s [7]. The exhaust fan was located at the downstream opening positioned below the transversal beam depth.

Table 4 shows that the critical velocity for the case of constant temperature boundary condition was much lower than that of adiabatic boundary condition. The hot gases would remain at the upper level if the critical velocity was low enough. The difference of critical velocity for the two cases was 0.14 m/s.

Table 4
The difference of critical velocity between constant temperature and adiabatic

Beam angular position	Constant temperature	Adiabatic
concave	0.03	0.14
30°	0.03	0.16
55°	0.02	0.13
60°	0.03	0.15
65°	0.03	0.13

4. Conclusions

Since not all information are available while designing the CFD model, this study intends to investigate the effect of different boundary condition towards heat release rate, smoke concentration, and temperature field as well as critical velocity which influence the occurrences of smoke back layering. Prior to examination, both grid and domain dependence studies were performed. The grid size of 0.94 cm was finally chosen. For heat release rate, it was found that the constant temperature boundary condition showed the higher R^2 (89.4%) than that of the adiabatic condition (87.5%). In the case of adiabatic condition, the smoke took lesser time to reach the floor level. Conversely, the tenability condition in the underground car park was met for the constant temperature boundary condition as the smoke remained longer at the upper level and less smoke was found near the end wall. Moreover, the temperature distribution near the ceiling was lower in the constant temperature boundary condition due to minimal buoyancy effect. The influence of critical velocity on the smoke layer was investigated as well. It was found that the critical velocity for the case employing constant temperature boundary condition was much lower than that of the adiabatic condition. As the intention of fire safety is to encourage the occupants to have longer time for escape by having the smoke to remain longer at the upper level, the constant temperature boundary condition should be used for the subsequent analysis.

Acknowledgement
This study work is supported by the scholarship provided by Malaysia Public Service Department to the first author.

References

[1] Klote, John H., and James A. Milke. *Principles of smoke management*. Atlanta, USA: American Society of Heating, Refrigerating and Air-Conditioning Engineers, 2002.
[2] Se, Camby MK, Eric WM Lee, and Alvin CK Lai. "Impact of location of jet fan on airflow structure in tunnel fire." *Tunnelling and Underground Space Technology* 27, no. 1 (2012): 30-40.
[3] Horváth, István, Jeroen van Beeck, and Bart Merci. "Full-scale and reduced-scale tests on smoke movement in case of car park fire." *Fire safety journal* 57 (2013): 35-43.
[4] Tilley, Nele, Xavier Deckers, and Bart Merci. "CFD study of relation between ventilation velocity and smoke backlayering distance in large closed car parks." *Fire Safety Journal* 48 (2012): 11-20.
[5] Sakr, Ismail M., Wageeh Ahmed El-Askary, Ashraf Balabel, and K. Ibrahim. "Computations of upward water/air fluid flow in vertical pipes." *CFD letters* 4, no. 4 (2012): 193-213.
[6] Morgan, H. P., B. Vanhove, and J. C. De Smedt. "Extending the principles of impulse ventilation in tunnels to apply to smoke control in car parks." *Int J Eng Perform Fire Code* 2 (2004): 53-71.
[7] Deckers, Xavier, S. Haga, Nele Tilley, and Bart Merci. "Smoke control in case of fire in a large car park: CFD simulations of full-scale configurations." *Fire Safety Journal* 57 (2013): 22-34.
[8] Jia, Fuchen, Zhaozhi Wang, and Edwin R. Galea. "Modelling factors that influence CFD fire simulations of large tunnel fires." (2010): 1091-1102.
[9] Mukhtar, A., K. C. Ng, and M. Z. Yusoff. "Design optimization for ventilation shafts of naturally-ventilated underground shelters for improvement of ventilation rate and thermal comfort." *Renewable Energy* 115 (2018): 183-198.
[10] Johansson, N. "Numerical experiments and compartment fires, Fire Sci." (2014).
[11] Hwang, Cheol-Hong, Andrew Lock, Matthew Bundy, Erik Johnsson, and Gwon Hyun Ko. "Studies on fire characteristics in over-and underventilated full-scale compartments." *Journal of fire sciences* 28, no. 5 (2010): 459-486.
[12] Beji, Tarek, Sebastian Ukleja, Jianping Zhang, and M. A. Delichatsios. "Fire behaviour and external flames in corridor and tunnel-like enclosures." *Fire and Materials* 36, no. 8 (2012): 636-647.
[13] Meng, Na, Longhua Hu, Shi Zhu, and Lizhong Yang. "Effect of smoke screen height on smoke flow temperature profile beneath platform ceiling of subway station: An experimental investigation and scaling correlation." *Tunnelling and Underground Space Technology* 43 (2014): 204-212.

[14] Hu, L. H., L. F. Chen, and W. Tang. "A global model on temperature profile of buoyant ceiling gas flow in a channel with combining mass and heat loss due to ceiling extraction and longitudinal forced air flow." *International Journal of Heat and Mass Transfer* 79 (2014): 885-892.
[15] Lu, S., Y. H. Wang, R. F. Zhang, and H. P. Zhang. "Numerical study on impulse ventilation for smoke control in an underground car park." *Procedia Engineering* 11 (2011): 369-378.
[16] Zhang, Bosi, Jiaqing Zhang, Shouxiang Lu, and Changhai Li. "Buoyancy-driven flow through a ceiling aperture in a corridor: A study on smoke propagation and prevention." In *Building Simulation*, vol. 8, no. 6, pp. 701-709. Tsinghua University Press, 2015.
[17] Meroney, Robert N., Douglas W. Hill, Russ Derickson, Jim Stroup, Ken Weber, and Peter Garrett. "CFD simulation of ventilation and smoke movement in a large military firing range." *Journal of Wind Engineering and Industrial Aerodynamics* 136 (2015): 12-22.
[18] Ji, J., Y. Y. Fu, C. G. Fan, Z. H. Gao, and K. Y. Li. "An experimental investigation on thermal characteristics of sidewall fires in corridor-like structures with varying width." *International Journal of Heat and Mass Transfer* 84 (2015): 562-570.
[19] Siang, Chan Chau. "Characterizing smoke dispersion along beamed ceilings using salt-water modeling." PhD diss., University of Maryland, College Park, 2010.
[20] Delichatsios, Michael A. "The flow of fire gases under a beamed ceiling." *Combustion and Flame* 43 (1981): 1-10.
[21] Santoso, Muhammad Agung, Zilvan Bey, and Yulianto Sulistyo Nugroho. "CFD study on the ventilation system and shape configuration of underground car park in case of fire." *Applied Mechanics & Materials* 758 (2015).
[22] Vettori, Robert L. *Effect of Beamed, Sloped, and Sloped Beamed Ceilings on the Activation Time of a Residential Sprinkler*. National Institute of Standards and Technology, Building and Fire Research Laboratory, 2003.
[23] Deckers, Xavier, S. Haga, Bart Sette, and Bart Merci. "Smoke control in case of fire in a large car park: Full-scale experiments." *Fire Safety Journal* 57 (2013): 11-21.
[24] Celik, Ishmail B., Urmila Ghia, and Patrick J. Roache. "Procedure for estimation and reporting of uncertainty due to discretization in {CFD} applications." *Journal of fluids {Engineering-Transactions} of the {ASME}* 130, no. 7 (2008).
[25] Kozić, Mirko. "Influence of thermal boundary conditions in a numerical simulation of a small-scale tunnel fire." *Scientific Technical Review* 59, no. 2 (2009): 18-23.
[26] Fišer, Jan, Jan Jedelský, Tomáš Vach, Matěj Forman, and Miroslav Jícha. "Comparison of CFD simulations and measurements of flow affected by coanda effect." In *EPJ Web of Conferences*, vol. 25, p. 01015. EDP Sciences, 2012.
[27] BS 7346-7, Components for smoke and heat control systems. Code of practice on functional recommendations and calculation methods for smoke and heat control systems for covered car parks, BSI Standard Limited 2013, 2013.
[28] Hansen, Rickard, and Haukur Ingason. "Model scale fire experiments in a model tunnel with wooden pallets at varying distances." (2010).